Journal of Porphyrins and Phthalocyanines
J. Porphyrins Phthalocyanines **2**, 391–396 (1998)

Synthesis and Crystal Structure of 5,10,15,20-Tetrakis(3,5-dinitrophenyl)porphyrin†

P. BHYRAPPA and K. S. SUSLICK*

Department of Chemistry, University of Illinois at Urbana-Champaign, 601 South Goodwin Avenue, Urbana, IL 61801, USA

Received 15 August 1997
Accepted 11 February 1998

ABSTRACT: The synthesis, characterization and crystal structure of the octanitro-substituted porphyrin 5,10,15,20-tetrakis(3,5-dinitrophenyl)porphyrin, H_2T(3,5-DNP)P, are described. The solid state structure has two porphyrins in the unit cell with eight pyridine solvates and is made up from columnar arrays of the porphyrins. X-ray crystal structure data: monoclinic, space group $P1\,2_1/n1$, a = 14.9996(9) Å, b = 8.2489(5) Å, c = 24.818(2) Å, $\alpha = 90°$, $\beta = 104.172(1)°$, $\gamma = 90°$, V = 2977.3(3) Å^3, d_{calc} = 1.440 g m^{-3}, Z = 2. © 1998 John Wiley & Sons, Ltd.

KEYWORDS: tetraphenylporphyrin; tetraarylporphyrin; nitroporphyrin; synthesis; X-ray crystallography; structure determination

INTRODUCTION

Syntheses of molecular synthons are of considerable interest in the design of molecular solids with desired applications [1–5]. Highly substituted *meso*-tetraarylporphyrins are an interesting class of molecular building blocks owing to their large size, extended π-system and versatility of metal ion binding. Furthermore, the peripheral phenyl rings can be used to provide three-dimensional orientations of a variety of functional groups. For example, tetraphenylporphyrins are capable of forming clathrate-like host/guest complexes [6–8]. An extensive crystallographic examination of solid state structures of porphyrins and metalloporphyrins reveals a wide range of interesting intermolecular interactions [9]. Specific design of functionalized porphyrins can lead to even more general control of crystal interactions. Notably, several supramolecular architectures of porphyrinic solids with hydrogen-bonded [10–12] or metal–organic coordination [13, 14] networks have been reported over the past few years.

Recently we have reported a series of octahydroxy tetraphenylporphyrins as building blocks for designing hydrogen-bonded supramolecular networks [11, 12]. The structural motifs of the crystal structure of these materials are dramatically controlled by the position of the substituents, size of the solvates and choice of the coordinated metal ion. Incorporation of halogen substituents (Cl or Br) at the *meso*-phenyl positions of the porphyrin can also produce unusual intermolecular interactions [15, 16].

Herein we report the synthesis, characterization and X-ray crystal structure of a new type of metalloporphyrin building block, 5,10,15,20-tetrakis(3,5-dinitrophenyl)porphyrin, H_2T(3,5-DNP)P. The solid state structure of this porphyrin is made up from columnar arrays of the porphyrins with four pyridine solvates per porphyrin.

EXPERIMENTAL

Materials

All the solvents employed in the present study were of reagent grade and were distilled before use. Dichloromethane and pyridine were distilled over CaH_2 under N_2 before use. DMSO, quinoline, 3,5-dinitrobenzyl alcohol and chromium trioxide were obtained from Aldrich and used as received. Quinolinium chlorochromate was prepared using literature procedures [17, 18].

*Correspondence to: K. S. Suslick, Department of Chemistry, University of Illinois at Urbana-Champaign, 601 South Goodwin Avenue, Urbana, IL 61801, USA.
†In honor of Professor V. Krishnan on the occasion of his retirement.

CCC 1088–4246/98/040391–06 $17.50

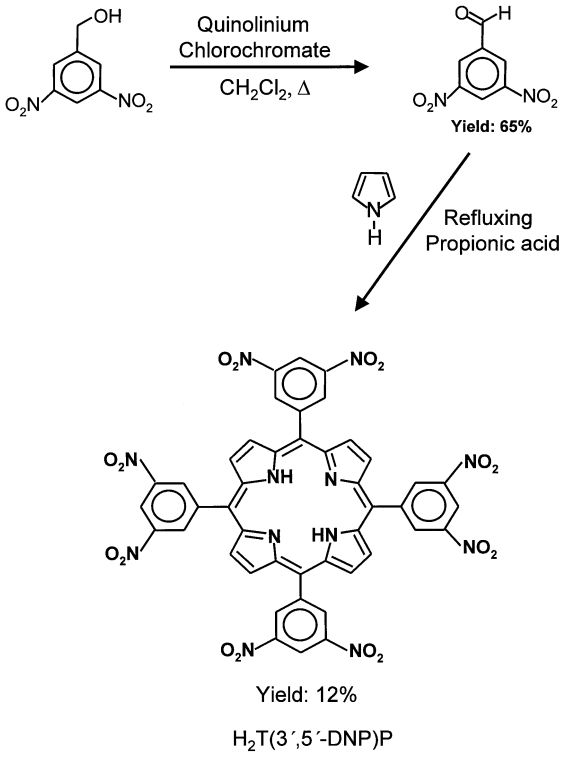

Scheme 1. Synthetic scheme for 3,5-dinitrobenzaldehyde and 5,10,15,20-tetrakis(3,5-dinitrophenyl)porphyrin, $H_2T(3,5\text{-DNP})P$.

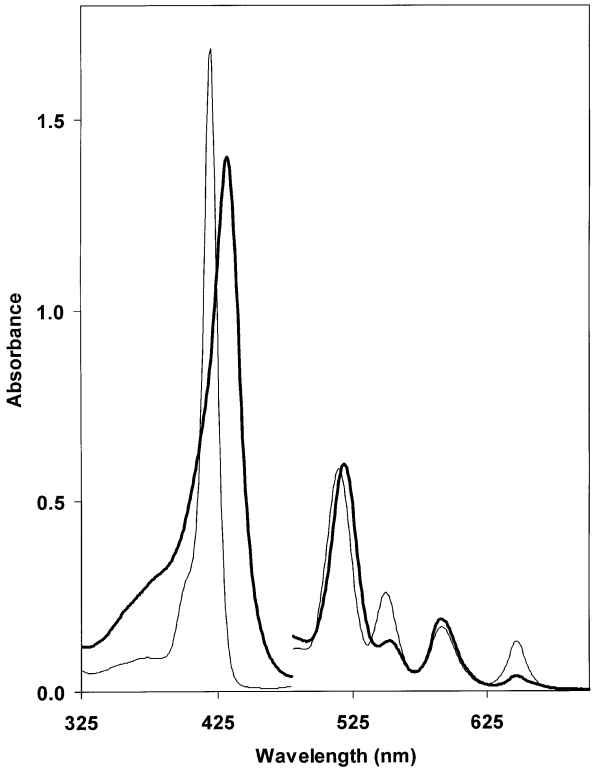

Fig. 1. Electronic absorption spectra of $H_2T(3,5\text{-DNP})P$ (thick line) and H_2TPP (thin line) in pyridine.

Synthesis of 3,5-Dinitrobenzaldehyde

This compound was synthesized in one step by the oxidation of dinitrobenzyl alcohol using quinolinium chlorochromate [17, 18] as the oxidant, as shown in Scheme 1. In a typical oxidation reaction, to a CH_2Cl_2 (100 mL) solution containing 3,5-dinitrobenzyl alcohol (5 g, 0.025 M), quinolinium chlorochromate (10 g, 0.038 M) solid was added slowly. The mixture was then stirred and refluxed for a period of 12 h. At the end of this period the solution was filtered and the solvent was evaporated to obtain an orange solid. The residue thus obtained was redissolved in the minimum amount of CH_2Cl_2 and chromatographed on a silica gel column using CH_2Cl_2 as the eluent. Then the first moving band was collected and the desired 3,5-dinitrobenzaldehyde was obtained on evaporation of the solvent. The yield of the product was 3.5 g (65%). ^{1}H NMR (DMSO-d_6): δ (ppm) 10.21 (s, H, aldehyde-H), 9.04 (t, H, *p*-H), 9.02 (d, 2H, *o*-H). Elemental analysis calc. for $C_7H_4N_2O_5$: C, 42.87; H, 2.06; N, 14.28%. Found: C, 42.97; H, 2.17; N, 13.96%.

Synthesis of 5,10,15,20-Tetrakis(3,5-dinitrophenyl)porphyrin, $H_2T(3,5\text{-DNP})P$

This porphyrin was synthesized using a variant of the Adler procedure [19], as shown in Scheme 1. Freshly distilled pyrrole (1.02 g, 0.015 mol) was added to a propionic acid solution (200 mL) containing 3,5-dinitrobenzaldehyde (3.0 g, 0.015 mol). The solution was refluxed and stirred for 6 h and allowed to cool to room temperature. Then the reaction mixture was filtered and the residue was washed with methanol until the filtrate was colorless. The residue was redissolved in the minimum amount of pyridine and chromatographed on a basic alumina column using pyridine as the eluent. The first moving band was collected to obtain the porphyrin. Finally, the porphyrin was recrystallized from pyridine/CH_2Cl_2 solvent mixture in a yield of 0.34 g (12%).

The free-base porphyrin $H_2T(3,5\text{-DNP})P$ was characterized by UV-vis (Fig. 1), ^{1}H NMR (Fig. 2), elemental analysis and mass spectroscopic techniques. UV-vis (pyridine): λ_{max} (nm) ($\log(\varepsilon/\text{mol}^{-1}\ \text{L cm}^{-1})$) 432 (5.83), 519 (4.43), 552 (4.07), 590 (3.87), 646

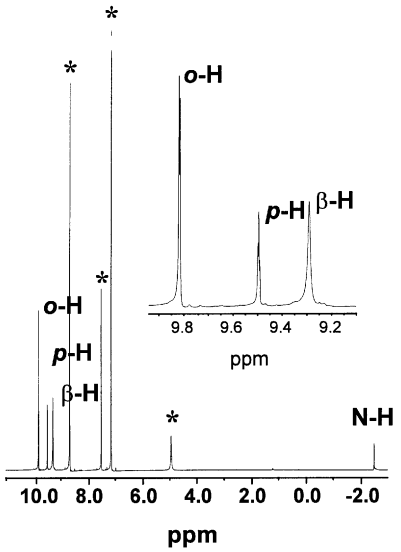

Fig. 2. ^{1}H NMR spectrum of H_2T(3,5-DNP)P in pyridine-d_5. Inset shows expanded region from 9.10 to 10.0 ppm. Starred peaks are solvent impurities.

(3.78). ^{1}H NMR (pyridine-d_5): δ (ppm) 9.82 (d, 8H, *o*-H), 9.50 (t, 4H, *p*-H), 9.29 (s, 8H, β-pyrrole-H), −2.49 (s, 2H, imino-H). Elemental analysis calc. for $C_{44}H_{22}N_{12}O_{16}$: C, 54.22; H, 2.27; N, 17.24%. Found: 53.98; H, 2.00; N, 16.98%. FAB mass spectrum (*m/z*): calc., 974.7; found, 975.2.

X-ray Data Collection and Refinement

The X-ray data were collected on an automated Siemens Smart-CCD diffractometer. A single crystal of the porphyrin H_2T(3,5-DNP)P was covered with oil (Paratone-N, Exxon), mounted on a thin glass fiber and cooled to 198 K. Intensity data were collected in ω–2θ mode in the range from 2.9° to 46° at 198 K.

The structure was solved by direct methods (SHELXL) [20]. The non-H atoms of the porphyrin macrocycle were obtained from the E-map. The structural analysis including one cycle of isotropic least-squares refinement by an unweighted Fourier difference synthesis revealed the positions of ordered atoms. The analysis involved full-matrix least-squares refinement on F^2 (SHELXL) and successful convergence was indicated by the maximum shift/error for the cycle [21]. Inversion symmetry was imposed on the host porphyrin molecule. Disordered pyridine solvate molecules were refined as rigid idealized groups. Thermal displacement parameters for disordered pyridine atom positions separated by less than 1.3 Å were restrained to equivalent values with an effective standard deviation of 0.01. Owing to the paucity of observed data at high angles, the resolution was limited to 0.90 Å. The space group choice was confirmed by successful convergence of the full-matrix least-squares refinement on F^2. The highest peaks in the final Fourier difference map were in the vicinity of the disordered pyridine solvate; the final map had no other significant features. A final analysis of variance between observed and calculated structure factors showed no dependence on amplitude or resolution. The final Fourier difference map showed residual electron density in the vicinity of the disordered pyridine solvates; the final map had no significant features.

RESULTS AND DISCUSSION

Synthesis and Characterization

For the synthesis of octanitro porphyrin, the precursor 3,5-dinitrobenzaldehyde was prepared by the facile oxidation of 3,5-dinitrobenzyl alcohol using the mild oxidizing agent quinolinium chlorochromate. H_2T(3,5-DNP)P was synthesized in moderate yields using the Adler procedure (Scheme 1). While H_2T(3,5-DNP)P is only very sparingly soluble in most organic solvents, it has good solubility in pyridine or triethylamine; H_2T(3,5-DNP)P is about 20% as soluble in pyridine as H_2TPP.

The UV-vis spectrum of H_2T(3,5-DNP)P, shown in Fig. 1 is a typical porphyrinic normal spectrum with four visible (Q) bands and an intense Soret (B) band. For H_2T(3,5-DNP)P the Q-bands show no significant shift, while the B-band is red-shifted by 12 nm relative to H_2TPP in pyridine. The Q_x(0,0)- and Q_y(0,0)-bands of H_2T(3,5-DNP)P are decreased in intensity relative to the Q_x(1,0)- and Q_y(1,0)-bands. The relative intensity pattern of the Q-bands of H_2T(3,5-DNP)P differs from that of H_2TPP and is similar to that of the perfluorinated porphyrin 5,10,15,20-tetrakis(2′,3′,4′,5′,6′-pentafluorophenyl)porphyrin, H_2(TFPP) [22]. Interestingly, H_2T(3,5-DNP)P shows a considerable broadening of the Soret band (full width at half-maximum, FWHM, 28 nm) relative to H_2TPP (FWHM 13 nm). This may be due to charge transfer interactions between the porphyrin and nitro aryl groups.

The ^{1}H NMR spectrum of H_2T(3,5-DNP)P is shown in Fig. 2. It features the characteristic proton resonances arising from pyrrole and *meso*-aryl groups.

Octanitro porphyrin shows a downfielded β-pyrrole resonance (9.28 ppm) relative to H_2TPP (8.9 ppm) in pyridine. Surprisingly, in $H_2T(3,5\text{-DNP})P$ the *meso*-phenyl proton signals appear downfield of the β-pyrrole resonance. The *ortho*- and *para*-phenyl proton resonances of $H_2T(3,5\text{-DNP})P$ appear as a doublet at 9.87 ppm (H_2TPP, 8.20 ppm) and as a triplet at 9.40 ppm (H_2TPP, $\sim$7.6 ppm) respectively. This downfield shift of the resonances of octanitro porphyrin is due to the inductive effect of the electron-withdrawing nitro groups on the aryl rings. The inner imino hydrogens appear as a singlet at -2.49 ppm, relative to -2.75 ppm for H_2TPP.

X-ray Structure of $H_2T(3,5\text{-DNP})P\cdot 4C_5H_5N$

Single crystals of $H_2T(3,5\text{-DNP})P\cdot 4C_5H_5N$ were grown by direct solvent diffusion of *n*-hexane in a saturated solution of the porphyrin in pyridine over a period of 3 days. The unit cell has two porphyrins with eight pyridine solvates. The pyridines show considerable disorder and were modeled as rigid idealized groups. The ORTEP diagram of $H_2T(3,5\text{-DNP})P\cdot 4C_5H_5N$ is shown in Fig. 3. The porphyrin ring is slightly ruffled compared with the structure of H_2TPP [19]. The observed bond lengths and bond angles of the porphyrin macrocycle are not significantly different from those of H_2TPP [23] or the corresponding hydroxy-substituted porphyrin 5,10,15,20-tetrakis(3,5-dihydroxyphenyl)porphyrin, $H_2(T(3,5\text{-DHP})P)\cdot 5EtOAc$ [11, 12]. The phenyl rings are almost planar and are oriented almost perpendicular to the porphyrin ring at an angle of 56.0°–68.5°, compared with 75.4°–91.1° for $H_2(T(3,5\text{-DHP})P)\cdot 5EtOAc$. The peripheral nitro groups are almost planar with the phenyl rings, with an O—N—O angle of 122°–124°.

The intermolecular packing diagram shown in Fig. 4 reveals a one-dimensional columnar structure for $H_2T(3,5\text{-DNP})P\cdot 4C_5H_5N$. The porphyrins are arranged in a columnar fashion with an inter-porphyrin vertical distance of 7.40(1) Å . This indicates minimal π–π interactions between the porphyrins. The O—O distance between the nitro groups of adjacent porphyrins within a column is 3.22(1) Å. This indicates only minimal interactions between the nitro groups, unlike those observed in 1,3,5-trinitrobenzene structures [24]. The closest distance between the aryl group carbon and the nitro group oxygen of adjacent porphyrins within a column is 3.57(1) Å. The phenyl rings are arranged in an offset fashion between the columns. The closest inter-nuclear distance between the aryl group carbon and the nitro group oxygen between two columns is 3.41(1) Å. The phenyl rings of adjacent porphyrins are offset and the closest distance between the phenyl rings of adjacent columns is 3.90(1) Å, indicating minimal π–π interactions.

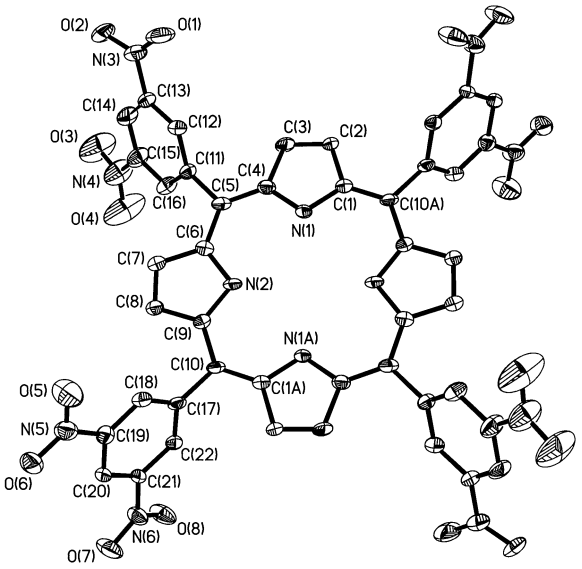

Fig. 3. ORTEP diagram of $H_2T(3,5\text{-DNP})P\cdot 4C_5H_5N$ with 35% thermal ellipsoids. Hydrogen atoms and pyridine solvates are omitted for clarity.

A space-filled molecular packing diagram of $H_2T(3,5\text{-DNP})P\cdot 4C_5H_5N$ is shown in Fig. 5. The columns are arranged front and back alternately, with a center-to-center distance of about 15.0 Å . There is a solvate-filled channel of about 4.0 Å by 3.6 Å running between the columns. The oxygen atom of the nitro group of one porphyrin faces the center of the phenyl ring of another porphyrin in the adjacent column. The distance between the aryl-nitro oxygen and the adjacent porphyrin aryl-carbon is rather short, 2.89(1) Å . Thus this solid state structure is stabilized by unusual aryl-ONO—C (aryl) intermolecular and van der Waals forces rather than by any strong nitro–nitro or π–π interactions.

CONCLUSIONS

A new type of metalloporphyrin building block, 5,10,15,20-tetrakis(3,5-dinitrophenyl)porphyrin, has been synthesized and fully characterized. We find that the solid state structure of this porphyrin comprises columnar stacks of the porphyrins with unusual aryl-ONO—C (aryl) intermolecular and van

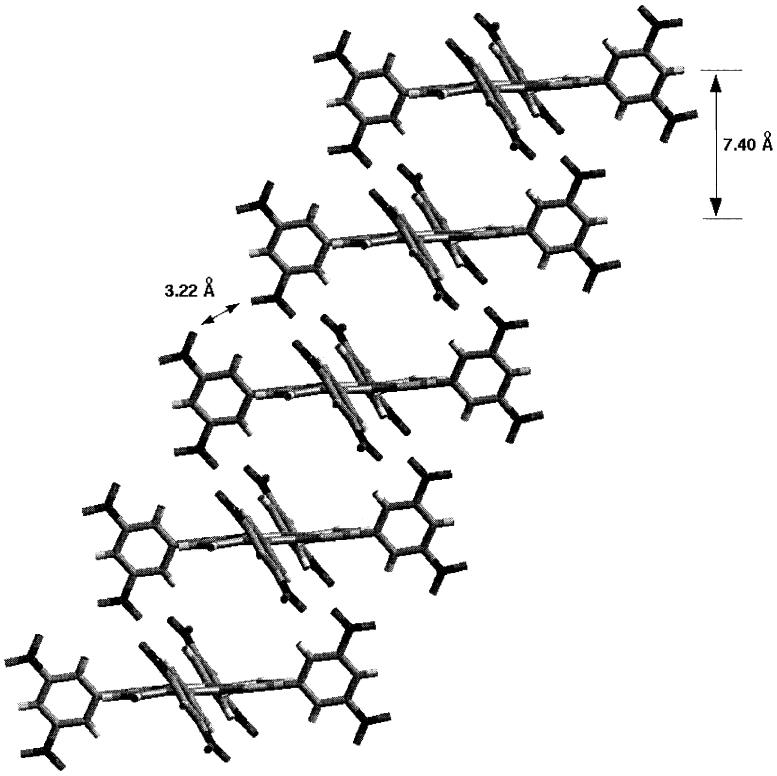

Fig. 4. One-dimensional columnar packing diagram of $H_2T(3,5\text{-DNP})P{\cdot}4\ C_5H_5N$. Pyridine solvates are omitted for clarity.

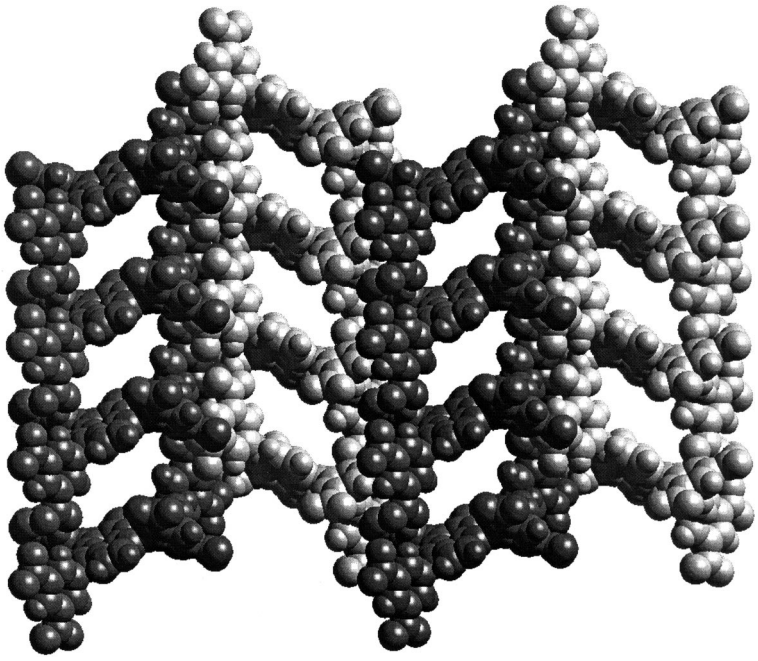

Fig. 5. Molecular packing diagram of $H_2T(3,5\text{-DNP})P{\cdot}4\ C_5H_5N$ complex shown along 001 plane. Space filling is shown at 0.7 of van der Waals atomic radii. The porphyrins shown in dark and light shades are closer and farther away respectively. Pyridine solvates are omitted for clarity.

der Waals interactions. A clathrate host/guest complex of four strongly held pyridines per porphyrin is present in the structure. This porphyrin is an important intermediate in the formation of other highly functionalized porphyrins and will prove useful in the synthesis of novel dendrimer complexes for a variety of applications [25, 26].

SUPPORTING INFORMATION

Crystallographic data on $H_2T(3,5\text{-DNP})P\cdot 4C_5H_5N$ including atomic positions, bond distances, torsion angles and bond angles (13 pages) and observed and calculated structure factors (10 pages) are available.

Acknowledgements

We thank Dr Scott R. Wilson and Theresa Prussek for helping in X-ray structure determination. This work was supported by the National Institute of Health (HL 5R01-25934) and in part by the US Army Research Office (DAAG55-97-0126) and the Dept. of Energy (ER45439).

REFERENCES AND NOTES

1. S. Komarneni, D. M. Smith and J. S. Beck (eds), *Advances in Porous Materials*, Materials Research Society, Pittsburgh, PA (1995).
2. T. Bein (ed.), *ACS Symp. Ser.* **499**, 88–253 (1992).
3. O. M. Yaghi, G. Li and H. Li, *Nature* **378**, 703 (1995).
4. D. Venkataraman, G. B. Gardner, S. Lee and J. S. Moore, *J. Am. Chem. Soc.* **117**, 11 600 (1995).
5. O. M. Yaghi, L. Hailian and T. L. Groy, *J. Am. Chem. Soc.* **118**, 9096 (1996) and references cited therein.
6. M. P. Byrn, C. J. Curtis, Y. Hsiou, S. I. Khan, P. I. Sawin, S. K. Tendick, A. Terzis and C. E. Strouse, *J. Am. Chem. Soc.* **115**, 9480 (1993).
7. H. Krupitsky, Z. Stein and I. Goldberg, *J. Inclu. Phenom.* **20**, 211 (1995).
8. H. Krupitsky, Z. Stein and I. Goldberg, *J. Inclu. Phenom.* **18**, 177 (1994).
9. W. R. Scheidt and Y. J. Lee, *Struct. Bond. (Berlin)* **64**, 1 (1987).
10. I. Goldberg, H. Kruptisky, Z. Stein, Y. Hsiou and C. E. Strouse, *Supramol. Chem.* **4**, 203 (1995).
11. P. Bhyrappa, S. R. Wilson and K. S. Suslick, *Supramol. Chem.* (1998).
12. P. Bhyrappa, S. R. Wilson and K. S. Suslick, *J. Am. Chem. Soc.* **119**, 8492 (1997).
13. B. F. Abrahams, B. F. Hoskins, D. M. Michall and R. Robson, *Nature* **369**, 727 (1994).
14. B. F. Abrahams, B. F. Hoskins, D. M. Michall and R. Robson, *J. Am. Chem. Soc.* **113**, 3606 (1991).
15. P. Dastidar, H. Krupitsky, Z. Stein and I. Goldberg, *J. Inclu. Phenom.* **24**, 241 (1996).
16. H. Krupitsky, Z. Stein and I. Goldberg, *J. Inclu. Phenom.* **20**, 211 (1995).
17. B. Ozgun and N. Degirmenbasi, *Synth. Commun.* **26**, 3601 (1996).
18. R. Srinivasan, C. V. Ramesh, W. Madhulatha and K. Balasubramanian, *Indian J. Chem. B* **35**, 480 (1996).
19. A. D. Adler, F. R. Longo, J. D. Finarelli, J. Goldmacher, J. Assour and L. Korsakoff, *J. Org. Chem.* **32**, 476 (1967).
20. G. M. Sheldrick, *SHELXL-93, Program for the Refinement of Crystal Structures from Diffraction Data*, University of Göttingen (1993).
21. Crystal data for $C_{64}H_{42}N_{16}O_{16}$ at 198 K: monoclinic, space group $P12_1/n1$, $a = 14.9996(9)$ Å, $b = 8.2489(5)$ Å, $c = 24.818(2)$ Å, $\alpha = 90°$, $\beta = 104.172(1)°$, $\gamma = 90°$, $V = 2977.3(3)$ Å^3, $d_{calc} = 1.440$ g m^{-3}, $Z = 2$, λ (Mo Kα) = 0.71073 Å, $2\theta_{max} = 46°$, R (obs. data) = 0.1251, wR (all data) = 0.2101 for 4040, 4142 unique, $2340 > 2\sigma(I)$, refinement based on F^2.
22. P. J. Spellane, M. Gouterman, A. Antipas, S. Kim and Y. C. Liu, *Inorg. Chem.* **19**, 386 (1980).
23. S. J. Silvers and A. Tulinsky, *J. Am. Chem. Soc.* **89**, 3331 (1967).
24. G. R. Desiraju, *Angew. Chem. Int. Ed. Engl.* **34**, 2311 (1995).
25. P. Bhyrappa, J. K. Young, J. S. Moore and K. S. Suslick, *J. Am. Chem. Soc.* **118**, 5708 (1996).
26. P. Bhyrappa, J. K. Young, J. S. Moore and K. S. Suslick, *J. Mol. Catal. A* **113**, 109 (1996).

